

Ultrafast dynamics in the vicinity of quantum light-induced conical intersections

András Csehi(1),(2), Markus Kowalewski (3) Gábor J. Halász(4), and Ágnes Vibók(1),(2)*,[†]

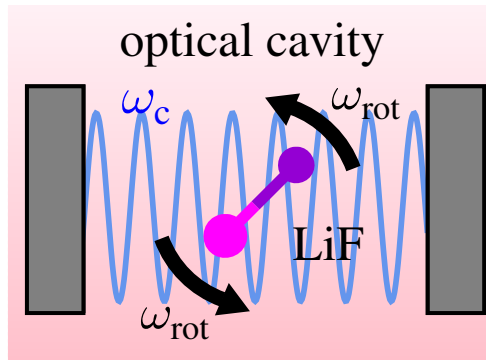
[†](1)*Department of Theoretical Physics, University of Debrecen, H-4002 Debrecen, PO Box 400, Hungary*

[‡](2)*ELI-ALPS, ELI-HU Non-Profit Ltd, H-6720 Szeged, Dugonics tér 13, Hungary*

[¶](3)*Department of Physics, Stockholm University, AlbaNova University Centre 106 91 Stockholm, Sweden*

[§](4)*Department of Information Technology, University of Debrecen, H-4002 Debrecen, PO Box 400, Hungary*

E-mail: vibok@phys.unideb.hu



For Table of Contents Only.

Abstract

Nonadiabatic effects appear due to avoided crossings or conical intersections that are either intrinsic properties in field-free space or induced by a classical laser field

in a molecule. It was demonstrated that avoided crossings in diatomics can also be created in an optical cavity. Here, the quantized radiation field mixes the nuclear and electronic degrees of freedom creating hybrid field-matter states called polaritons. In the present theoretical study we go further and create conical intersections in diatomics by means of a radiation field in the framework of cavity quantum electrodynamics (QED). By treating all degrees of freedom, that is the rotational, vibrational, electronic and photonic degrees of freedom on an equal footing we can control the nonadiabatic quantum light-induced dynamics by means of conical intersections. First, the pronounced difference between the the quantum light-induced avoided crossing and the conical intersection with respect to the nonadiabatic dynamics of the molecule is demonstrated. Second, we discuss the similarities and differences between the classical and the quantum field description of the light for the studied scenario.

Keywords: optical and microwave cavities; Fock states; population transfer; nonadiabatic couplings; light-induced conical intersections;

The dynamics initiated in a molecule by absorbing a photon is often described in the Born-Oppenheimer (BO) or adiabatic approximation¹, where the electronic and nuclear degrees of freedom are treated separately. However, in some nuclear configurations called conical intersections (CIs) the mixing between the electronic and nuclear motions are very significant²⁻⁶. Owing to the strong nonadiabatic couplings in the close vicinity of these CIs the BO approximation breaks down. It is well-known that these CIs have a significant impact on several important photo-dynamical processes, such as vision, photosynthesis, molecular electronics, and the photochemistry of DNA⁷⁻¹¹. During the dynamics the CIs can serve as efficient decay channels for the ultrafast transfer of the populations. In the following we call these CIs, which originate from the field free electronic structure, natural CIs.

Nonadiabatic effects can also appear when molecules are exposed to resonant laser

light. The electric field can couple to two or more electronic states of the molecule via the non-vanishing transition dipole moment(s) (TDMs)^{12–15}. This results either in a light-induced avoided crossing (LIAC) or a light-induced conical intersection (LICI) depending on how many nuclear degrees of freedom are involved in the field induced process¹⁶. In case of poly atomic molecules a sufficient number of vibrational degrees of freedom are always present to span a two-dimensional branching space (BS), which is indispensable to the formation of LICI. In the case of diatomics one always has to find a proper second degree of freedom which can act as a dynamical variable to form a BS. As the molecule rotates [17–19], the rotational angle between the molecular axis and the light polarization axis can serve as the missing degree of freedom for establishing the BS²⁰.

Nonadiabatic effects can arise in an optical or microwave cavity as well^{21–25}. Describing the photon-matter interaction with the tool of cavity quantum electrodynamics (cQED) is an emerging field. It has been successfully demonstrated both experimentally^{26–32} and theoretically^{33–49}, that the quantized photonic mode description of the electromagnetic field can provide an alternative solution for studying adequately the light-molecule’s quantum control problem. In this framework the nonadiabatic dynamics arises due to the strong coupling between the molecular degrees of freedom and the photonic mode of the radiation field which can alter the molecular levels by controlling the dynamics of basic photophysical and photochemical processes.

In most of the theoretical descriptions the molecules are treated via a reduced number of degrees of freedom or by some simplified models assuming two-level systems. Here, only one vibrational mode which is strongly coupled to the electronic and photonic degrees of freedom is taken into account resulting in a new set of “cavity induced” or “polariton” surfaces in the molecular Hamiltonian^{21–25}. These polariton surfaces can form CIs under special conditions²³ but are not expected to cross each other in general forming only “avoided crossings”. This scenario resembles a one-dimensional (1D), semi-classical treatment of the light-induced avoided crossing occurring in the nonadiabatic gas-phase molecular dynamics. Recent studies of the time-dependent state population in the NaI molecule have successfully demonstrated that the 1D results obtained by the semi-classical approach⁵⁰

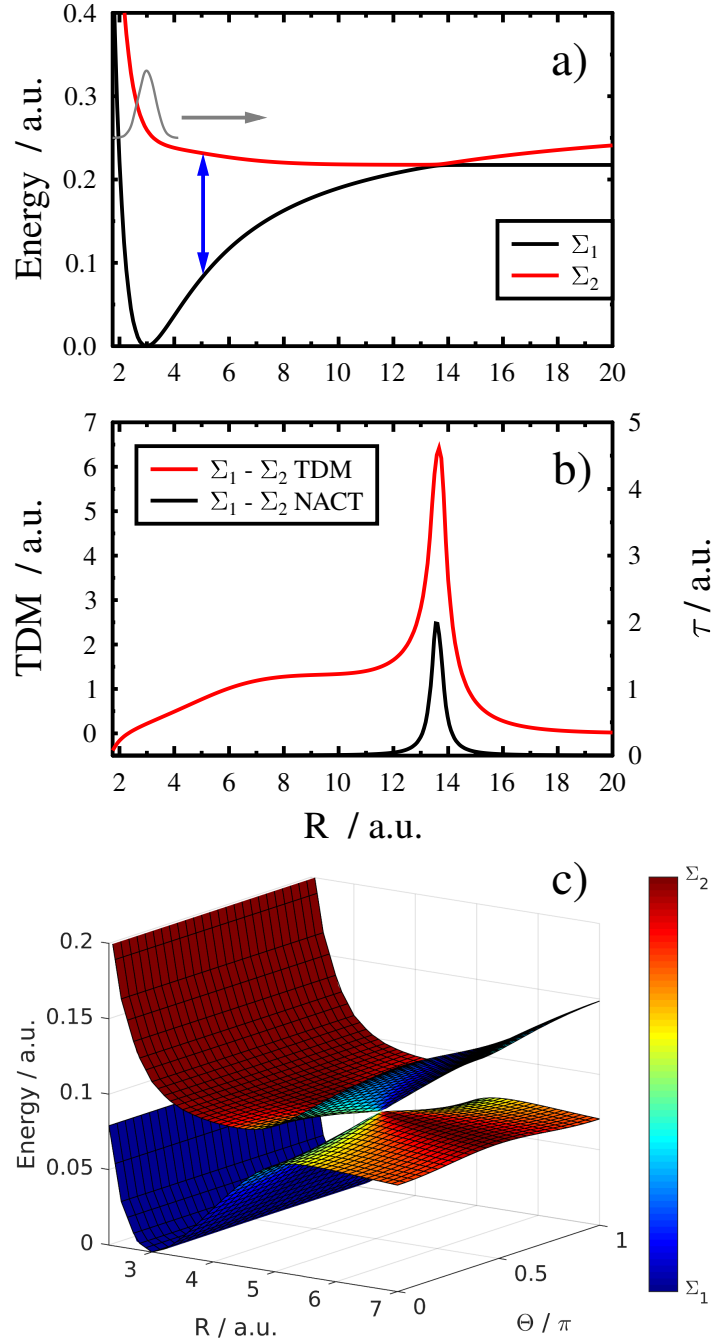


Figure 1: (a) Bare ground Σ_1 (black line) and excited Σ_2 (red line) electronic potential energy curves of the LiF molecule. The initial wave packet around $R = 3$ a.u. is indicated by the gray line while the resonant coupling of the electronic states at $R = 5$ a.u. is indicated by the vertical blue arrow. (b) Transition dipole moment (green line) and intrinsic nonadiabatic coupling (red line) functions of the Σ_1 and Σ_2 electronic states. (c) Dressed states potential energy surfaces of the LiF molecule representing the quantum light-induced CI for a cavity coupling $\chi = 0.02$ and a cavity resonance frequency $\omega_c = 0.1468$ a.u.. The color code indicates the state character in the terms of the bare states $|\Sigma_1, n + 1\rangle$ and $|\Sigma_2, n\rangle$. The LICI is located at $\theta = \pi/2$.

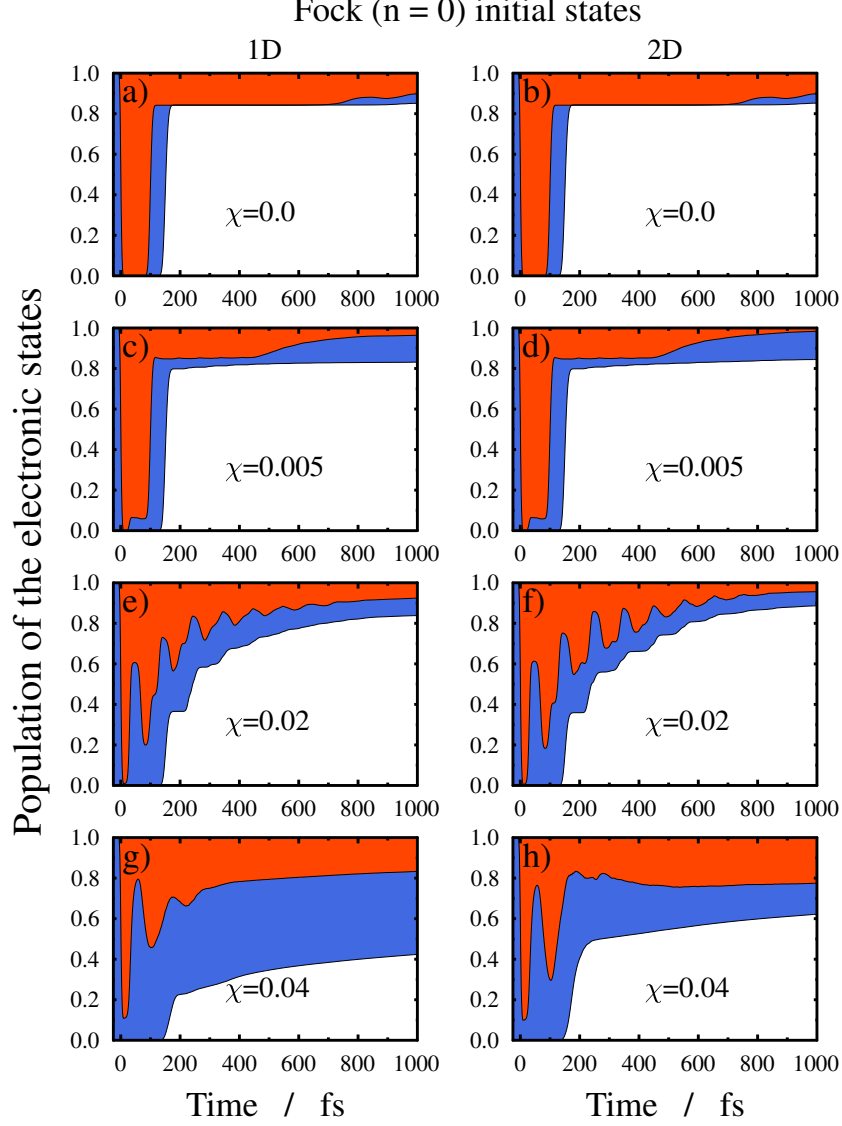


Figure 2: Population of the ground and excited electronic states as a function of time computed in 1D and 2D. Panels on the left-hand side (a)-g)) show the 1D results, while those on the right-hand side (b)-h)) depict the 2D results for a given cavity coupling strength; from top to bottom $\chi=0$, $\chi=0.005$, $\chi=0.02$ and $\chi=0.04$. The blue and red areas correspond to the population of the Σ_1 and the Σ_2 states, respectively. The white regions show the ground state population being in the dissociation region ($R > 20$ a.u.). In all the panels the Fock vacuum state ($n = 0$) is considered as an initial state along the cavity mode.

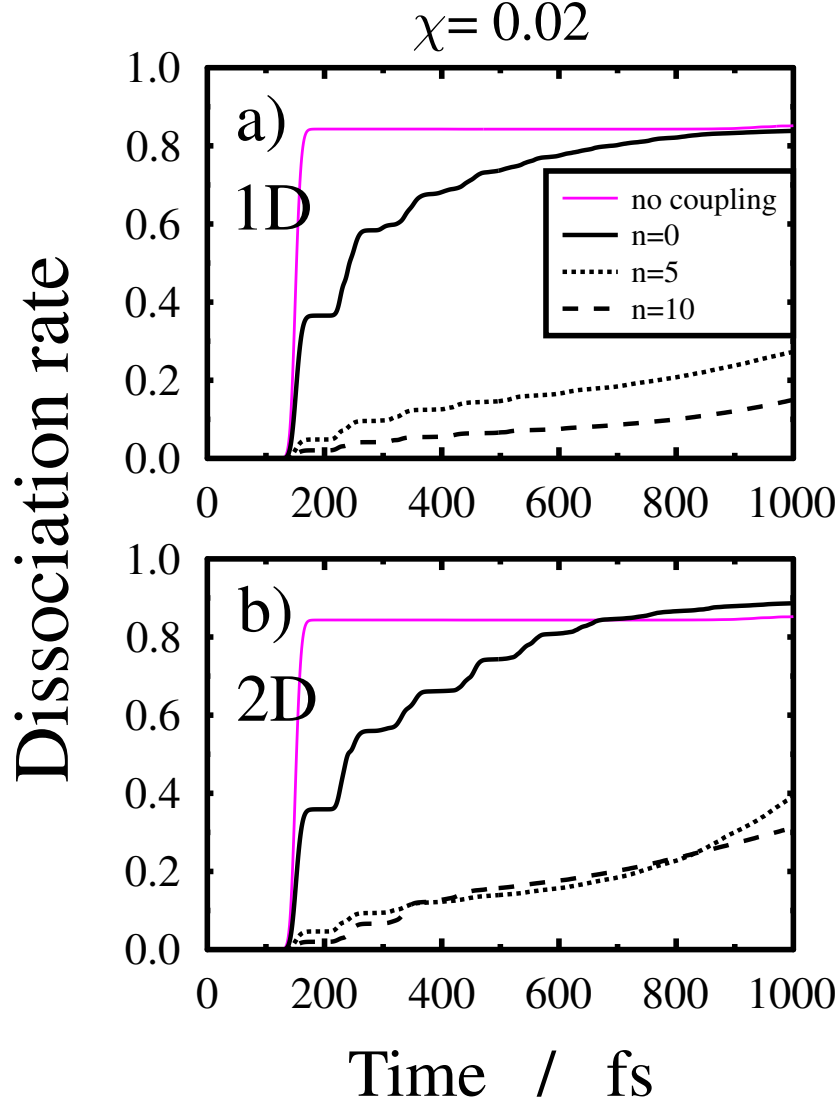


Figure 3: Time-evolution of the ground state dissociation rate for the LiF molecule considering different initial Fock states along the cavity mode. 1D and 2D results are compared in panels a) and b), respectively for a given cavity coupling strength of $\chi=0.02$. Besides the different photon number Fock states, the field-free results are shown by the magenta curves.

are fully consistent with the results obtained for NaI and quantized light field²⁴.

Adding another molecular degree of freedom, which can either be a second vibrational mode in case of poly atomics or the rotational angle between the molecular axis and the polarization axes in the cavity, one can fully describe the photon-induced quantum dynamics in the framework of quantum light-induced conical intersection (LICI). CIs can even be formed in diatomics due to the availability of the two independent nuclear degrees of freedom, which are essential for forming a 2D branching space. This picture can now be extended in a straightforward way from the simplified 1D model with a second molecular mode to treat the rotational, vibrational, electronic and photonic degrees of freedom on an equal footing. In the following we call the latter description the 2D description.

By including the molecular rotation in the cavity treatment, recently we have investigated the field-dressed rovibronic spectrum of diatomics in the framework of cavity quantum electrodynamics⁵¹. Incorporating the concept of LICIs with the quantized radiation field, similar impact on the adiabatic spectrum has been found as in the case of classical dressed situation⁵². We have demonstrated that the “intensity borrowing” effect can cause a significant variation in the pattern of the molecular spectra irrespective of the origin of the conical intersections. It can be either natural or light-induced and the latter can be created by classical or quantum light.

In the present work we go further and investigate theoretically how the dynamics of the lithium fluoride molecule, which already possesses a natural avoided crossing, is affected by quantum light-induced CI. This work complements previous theoretical investigations^{24,50}, where only avoided crossings were created by quantum light²⁴, but not CIs⁵⁰. Here we investigate the nonadiabatic quantum dynamics by incorporating the concept of LICIs with the quantized radiation field.

The aim of this letter is two-fold. First, we would like to study the quantum light-induced nonadiabatic dynamics of the LiF molecule both in 1D and 2D frameworks to demonstrate the difference between the effects of the radiation field-induced avoided crossing (AC) and CI. The underlying dynamics is mainly governed by the interplay between one of the quantum light-induced phenomena (either LIAC or LICI) and of

the natural avoided crossing which is present in the field-free molecule. Second, the similarities and the differences between the classical and the cavity Fock radiation field description of the light are investigated. We discuss for both the LIAC and LICI to what extent the different physical scenarios, a molecule in a laser field and a molecule in a cavity, show similar or different results.

The general form of the Hamiltonian in the basis of the adiabatic potential energy surfaces (PES) surfaces Σ_1 and Σ_2 of LiF can be given as

$$\begin{aligned} \hat{H}_{cavity} = & \left(-\frac{1}{2M_r} \frac{\partial^2}{\partial R^2} + \frac{1}{2M_r R^2} L_\theta^2 \right) \mathbf{1} + \begin{pmatrix} V_{\Sigma_1} & K \\ -K & V_{\Sigma_2} \end{pmatrix} + \left(-\frac{1}{2} \frac{\partial^2}{\partial x^2} + \frac{1}{2} \omega_c^2 x^2 \right) \mathbf{1} \\ & + \begin{pmatrix} \chi \omega_c \sqrt{2} \cdot \mu_{\Sigma_1} \cos \theta \cdot x & \chi \omega_c \sqrt{2} \cdot \mu_{\Sigma_1 \Sigma_2} \cos \theta \cdot x \\ \chi \omega_c \sqrt{2} \cdot \mu_{\Sigma_1 \Sigma_2} \cos \theta \cdot x & \chi \omega_c \sqrt{2} \cdot \mu_{\Sigma_2} \cos \theta \cdot x \end{pmatrix}. \end{aligned} \quad (1)$$

Here we assume the electric dipole approximation and that the molecule interacts with only a single mode of the cavity. In eq. 1, the first term represents the rovibrational kinetic energy of the LiF molecule with R and θ being the vibrational and rotational degrees of freedom, respectively. M_r is the reduced mass of the LiF molecule, L_θ is the angular momentum operator (with $m = 0$ fixed) and the $\mathbf{1}$ symbol represents the 2×2 unit matrix. The second term contains the field-free adiabatic potential curves V_{Σ_1} and V_{Σ_2} (see Fig. 1(a)). The K field-free nonadiabatic coupling operator is approximated as $K(R) \approx \frac{1}{2M_r} (2\tau(R) \frac{\partial}{\partial R} + \frac{\partial}{\partial R} \tau(R))$, where $\tau(R)$ is first order nonadiabatic coupling term, shown in Fig. 1(b). The third term in eq. 1 represents the harmonic oscillator description of the photon mode with the unit-less photon displacement coordinate x . Here ω_c is the cavity mode angular frequency. The last term of eq. 1 describes the interaction between the molecule and the quantized field. Here χ is the cavity coupling strength, while μ_i and μ_{ij} ($i, j = \Sigma_1, \Sigma_2$) are the permanent and transition dipoles, respectively. In the actual calculations $\hbar \omega_c = 3.995$ eV is taken which corresponds to the resonant coupling of the Σ_1 and Σ_2 states around $R=5$ a.u. The coupling strength χ ranges from 0.0012 to 0.04 to simulate moderate and strong coupling strengths.

The initial wave packet at $t = -10$ fs is created from the product of the rovibrational

ground state of Σ_1 located around $R \approx 3$ a.u. and one of the Fock states and is placed on the lower adiabatic potential Σ_1 . The Fock states are considered eigenstates of the $\left(-\frac{1}{2}\frac{\partial^2}{\partial x^2} + \frac{1}{2}\omega_c^2 x^2\right)$ Hamiltonian.

The form of the time-dependent Hamiltonian in the classical framework in the basis of the adiabatic states Σ_1 and Σ_2 of LiF reads:

$$\begin{aligned} \hat{H}_{classical}(t) = & \left(-\frac{1}{2M_r}\frac{\partial^2}{\partial R^2} + \frac{1}{2M_r R^2}L_\theta^2\right) \mathbf{1} + \begin{pmatrix} V_{\Sigma_1} & K \\ -K & V_{\Sigma_2} \end{pmatrix} \\ & - \varepsilon_0 \cdot \cos(\omega_c t) \cdot f(t) \begin{pmatrix} \mu_{\Sigma_1} \cos \theta & \mu_{\Sigma_1 \Sigma_2} \cos \theta \\ \mu_{\Sigma_1 \Sigma_2} \cos \theta & \mu_{\Sigma_2} \cos \theta \end{pmatrix}. \end{aligned} \quad (2)$$

In eq. 2, the first term represents the vibrational and rotational kinetic energy (the same as in eq. 1), while the second term contains the field-free V_{Σ_1} and V_{Σ_2} potential curves and the K nonadiabatic coupling operator. The third term of eq. 2 describes the laser-molecule interaction in the dipole approximation. Here ε_0 is the amplitude of the electric field, ω_c is the angular frequency of the laser, $f(t)$ is the envelope function which is set to unity during the whole propagation ($t_{final}=1000$ fs). μ_i and μ_{ij} ($i,j=\Sigma_1, \Sigma_2$) are the permanent and transition dipoles, respectively. The actual value of the applied laser energy was set to $\hbar\omega_c = 3.995$ eV, which resonantly couples the electronic states at $R = 5$ a.u., and the peak laser intensity ranges from $I_0 = 3 \times 10^{11}$ W/cm² to 3×10^{13} W/cm².

In both the cavity and classical calculations a linearly polarized resonant pump pulse is applied to initiate the dissociation dynamics. The form of this pump pulse is given as $\varepsilon_{pump} \cdot \cos(\omega_{pump} t) \cdot g(t)$ where ε_{pump} is the peak electric field strength, ω_{pump} is the resonance angular frequency and $g(t) = \cos^2(\frac{\pi t}{T_p})$ (in the $[-T_p/2, T_p/2]$ time interval) is the envelope function. Applying a laser pulse with a center frequency of $\hbar\omega_{pump} = 7$ eV, $T_p = 20$ fs pulse duration, and $I_{pump} = 4.8 \times 10^{13}$ W/cm² peak intensity, 35% of the total population is excited to Σ_2 . This wave packet then starts to oscillate and gradually dissociate on Σ_1 via the AC and LICI or LIAC.

The MCTDH (multi configurational time-dependent Hartree) method^{53,54} has been applied to solve the time-dependent Schrödinger-equation characterized by either eq. 1

or eq. 2. The R degree of freedom (DOF) was defined on a sin-DVR (discrete variable representation) grid (N_R basis elements for $R = 1.6 - 60$ a.u.). The rotational DOF, θ , was described by N_θ Legendre-polynomials, $P_l^m(\cos \theta)$ with $m = 0$ and $l = 0, 1, \dots, N_\theta - 1$. The photon displacement coordinate x was described by N_x Hermite-polynomials, $H_n(x)$ with $n = 0, 1, \dots, N_x - 1$. In the MCTDH wave function representation, these primitive basis sets (ξ) are then used to construct the single particle functions (ϕ) whose time-dependent linear combinations form the total nuclear wave packet (ψ)

$$\begin{aligned}\phi_{j_q}^{(q)}(q, t) &= \sum_{i=1}^{N_q} c_{j_q i}^{(q)}(t) \xi_i^{(q)}(q) \quad q = R, \theta, x \\ \psi(R, \theta, x, t) &= \sum_{j_R=1}^{n_R} \sum_{j_\theta=1}^{n_\theta} \sum_{j_x=1}^{n_x} A_{j_R, j_\theta, j_x}(t) \phi_{j_R}^{(R)}(R, t) \phi_{j_\theta}^{(\theta)}(\theta, t) \phi_{j_x}^{(x)}(x, t)\end{aligned}\tag{3}$$

The actual number of basis functions were $N_R = 1169$, $N_\theta = 271$ and $N_x = 100$ for the vibrational, rotational and photon modes, respectively. The number of single particle functions for the three DOFs and on both the Σ_1 and Σ_2 electronic states were ranging from 10 to 50. The values of $n_R = n_\theta$ and n_x were chosen depending on the actual value of the χ cavity coupling strength and I_0 peak laser intensity. In order to minimize unwanted reflexions and transmissions caused by the finite length of the R-grid, complex absorbing potentials (CAP) have been employed at the last 10 a.u. of the grid. The total propagation time was set to $t_{final} = 1000$ fs and the state populations and dissociation rates were calculated according to

$$P_i(t) = \langle \psi_i(R, \theta, x, t) | \psi_i(R, \theta, x, t) \rangle \quad i = \Sigma_1, \Sigma_2\tag{4}$$

and

$$P_{diss}(t) = \langle \psi_{\Sigma_1}(t) | \Theta(R - R_D) | \psi_{\Sigma_1}(t) \rangle + 2 \int_0^t dt' \langle \psi(t') | W | \psi(t') \rangle.\tag{5}$$

In eq. 5, Θ is the Heaviside step function, $R_D = 20$ a.u. is the starting point of the dissociation region, and $-iW$ is the CAP. To calculate the potential energy, the dipole moment, and the nonadiabatic coupling (NAC) curves of the LiF molecule (Fig. 1(b)), the program packages Molpro⁵⁵ was used. These quantities were calculated at the

MRCI/CAS(6/12)/aug-cc-pVQZ level of theory⁵⁶. In particular, $\tau(R)$ has been computed by finite differences of the MRCI electronic wave functions. The number of active electrons and molecular orbitals in the individual irreducible representations of the C_{2v} point group were $A_1 \rightarrow 2/5$, $B_1 \rightarrow 2/3$, $B_2 \rightarrow 2/3$, $A_2 \rightarrow 0/1$.

We start with the dynamics of the bare molecule (no cavity). Figures 2(a) and 2(b) show the time dependent populations of both the ground and excited states. The length of the red interval in vertical direction denotes the amount of the population in the excited states. The initial set up can be seen at $t < -10$ fs, when the whole population is on the ground state. Then a linearly polarized resonant pump pulse (the details of it are given in the introduction) is applied to initiate the dissociation dynamics. From now on all population will be related to the one which is transferred to the upper states during the pump process. The wave packet of the transferred population starts to oscillate on the excited state potential curve and reaches the avoided crossing at $t \approx 80$ fs. Here about 80% of the population is transferred back to the ground state due to the intrinsic nonadiabatic coupling. The area colored in blue shows the amount of the population on the ground state, which begins to dissociate at $t \approx 140$ fs. At $t \approx 180$ fs approximately 80% of the population dissociates (marked in white color) and does not show up again in the dynamics. In the bare molecule the Hamiltonians for 1D and 2D framework are effectively the same, which results in identical dynamics. The bumpy structure on the curves at $t \approx 800$ fs denotes that the wave packet has returned to the avoided crossing region.

By switching on the cavity coupling between the photonic and the molecular degrees of freedom, the quantum light-induced nonadiabaticity now competes with the intrinsic one. In the 1D calculations only the vibrational molecular degree of freedom mixes with the photonic mode and the electronic states, creating an avoided crossing between the polariton states. In the 2D scheme both the rotational and vibrational modes are accounted for and a LIC can be formed even for a diatomic molecule. We begin by investigating the vacuum state of the cavity mode ($n = 0$). We performed 1D and 2D calculations for several values of the cavity coupling and the results of the calculation

are shown in Fig. 2. It can be seen that with increasing coupling strength χ the 1D and 2D results increasingly deviate from each other and the impact of the LICI becomes more prominent. For a coupling parameter of ($\chi = 0.02$) large amplitude oscillations can be observed between the electronic surfaces both in the 1D and 2D populations. This is due to the increased splitting at the LIAC or LICI for larger coupling strengths creating decoupled dressed state surfaces^{21,23}. However, at the largest coupling parameter ($\chi = 0.04$), owing to the different shapes of the upper polaritonic surface in different directions. This period of this oscillation strongly depends on the molecular orientation which – after a few periods – leads to a wash out of the fingerprints of the oscillation from the total populations depicted in the figure. The dissociation itself is less suppressed in the cavity LICI picture than in the case of the quantum light-induced avoided crossing. This is clear evidence that in the cavity the bond hardening effect⁵⁷ is less efficient in 2D than in 1D. That is, even when the quantized radiation field couples to the molecular degrees of freedom, the ultrafast decay channel created by the LICI is more efficient with respect to the fast population transfer than the avoided crossing. Although the time evolution of the quantum dynamics is determined by the interplay between the radiation-field induced and intrinsic nonadiabaticity, at sufficiently strong coupling region the quantum LICI dominates the process. Similar effects have been found for natural avoided crossings, natural CIs, and for LIACs and LICIs induced by classical light field. In this work we have demonstrated the dynamics of quantum light-induced avoided crossings and quantum light-induced CIs for the first time.

To better understand the differences between the 1D and 2D results, we compare the dissociation rates for different photon number of Fock states ($n = 0, 5$, and 10) in Fig. 3. Again, the dissociation rate in the bare molecule ($\chi = 0$) is the same in 1D and 2D. However, for the vacuum Fock state ($n = 0$) a minor difference between the two schemes can be recognized. The structure of the dissociation curves is similar but the effect, that the dissociation is more efficient in 2D, can already be seen here. The efficiency of LICI is increasing compared to the 1D model when we use Fock states with $n = 5$ and $n = 10$ as an initial condition. Increasing the photon number of the initial state

the dissociation rate of the 2D model less suppressed than that of the 1D one. The decay channel provided by the quantum LICI is more efficient for transferring the population to the lower polaritonic state, which leads to higher dissociation rates. The effect is similar to what we experience in the case of increasing coupling strengths. Namely, the increasing photon number provides an increasing coupling strength, which is enhanced by $\sqrt{n+1}$, leading to a more efficient LICI. The rotation of the molecule starts slowly, therefore up to $t = 220$ fs the 1D and 2D curves are practically the same for all the studied photon number states. We now discuss Fig. 3(b) where we see two crossings between the $n = 5$ and $n = 10$ dissociation curves. Because the bond hardening effect is stronger for $n = 10$, evidently the dissociation starts slower. At $t = 330$ fs the effect of rotation suddenly becomes apparent resulting in crossings in the 2D curves (for $n = 5$ and 10). Between the period of $t = 350$ fs and $t = 850$ fs the rotation already plays an important role in amplifying the effect of the LICI. This effect is particularly pronounced for $n = 10$.

To gain more insight into this phenomena we have analyzed the two dimensional wave packet density functions $|\psi^{\Sigma_1}(R, \theta, t)|^2$, $|\psi^{\Sigma_2}(R, \theta, t)|^2$, $|\psi^{\Sigma_1}(x, \theta, t)|^2$, $|\psi^{\Sigma_2}(x, \theta, t)|^2$ and found that the $n = 5$ and $n = 10$ Fock states differ significantly from the $n=0$ vacuum. Namely, a much stronger alignment and bond hardening effect can be realized in the Fock space including photons than in the case of a vacuum which then strongly suppresses the dissociation rate. At weaker coupling strengths the dissociation rates obtained by the LICI and LIAC are more or less similar, independently from the photon number of the Fock states, while in the stronger coupling regime the LICI provides a significantly larger amount of dissociation rate. In the case of quantum light the molecular degrees of freedom interact directly with the photonic degrees of freedom and can modify the state of the light field through stimulated emission. This is not possible with a classical description of light field.

In Fig. 4 we compare the results of the cavity mode for a photon number $n = 5$ with the classical description as obtained from the 1D and 2D calculations. A similar comparison for the 1D model, but for a photon number $n = 0$, has been made between the quantum light and classical results of the Na_2 molecule ground state population⁵⁰.

This is comparable to our earlier findings where independently from the applied coupling strength practically no considerable difference has been found between the different 1D simulations. In contrast, in the 2D calculations significant differences have been found in the dissociation rates when comparing the classical and quantum light model. At weaker coupling strengths the difference is not so prominent, but becomes more significant at stronger couplings. At really short time dynamics the LIAC and LICI behave similarly but differ significantly at longer time scale.

In summary, we could show that the dynamical properties of diatomic molecules can be strongly modified by quantized light in an optical cavity. By using the LiF molecule as a showcase example, we demonstrated that the LICI created by quantum light allows for a more efficient population transfer than a LIAC given a sufficiently large coupling strength.. The stronger the cavity coupling, the more prominent the effect. This difference can be explained by the fact that the LICI retains a degeneracy between the dressed states even for large coupling strengths. In contrast, the dressed state curves of the 1D model become increasingly separated for larger coupling strengths, which leads to a decreased mixing between the nuclear degrees of freedom and the electron+photon degrees of freedom. In addition, for the case of LIAC a close similarity has been found between the classical and the cavity radiation field description of the light for all the studied coupling strengths and Fock states.

A significant difference has been found between the dynamics governed by the quantum Fock state and the classical light description of the LICI in the Hamiltonian. The stronger the coupling is, the larger difference becomes between the dynamics of the LICI formed by quantum and classical light. By increasing the coupling strength in the cavity description, the dissociation rate is more and more suppressed compared to the classical 2D calculation. It has also been realized that even in the quantum description of the LICI the photons which are present in the Fock state ($n = 5$ and $n = 10$) can also play an important role comparing to the Fock vacuum situation. The detailed dissection of the dynamics and the analysis of the interplay between photonic degrees and molecular degrees of freedom will be subject of a future study.

We note that there is more potential for exploring quantum LICIs in poly atomic molecules, covering a larger class of chemically relevant molecules. Here, the cavity induced nonadiabatic molecular dynamics can be studied in the absence of molecular rotations as they already provide the necessary number of vibrations to form CIs.

Acknowledgments

This research was supported by the EU-funded Hungarian grant EFOP-3.6.2-16-2017-00005. The authors are grateful to NKFIH for support (Grant K128396). M.K. acknowledges support from the Swedish Research Council (2018-05346).

References

- (1) Born M and Oppenheimer R 1927 *J. R. Ann. Phys.* **84** 457
- (2) Köppel H, Domcke W and Cederbaum L S 1984 *Adv. Chem. Phys.* **57** 59
- (3) Baer M 2002 *Phys. Rep.* **358** 75
- (4) Worth G A and Cederbaum L S 2004 *Annu. Rev. Phys. Chem.* **55** 127
- (5) Domcke W, Yarkony D R and Köppel H *Conical Intersections: Electronic Structure, Dynamics and Spectroscopy*; World Scientific, Singapore 2004
- (6) Baer M *Beyond Born Oppenheimer: Electronic Non-Adiabatic Coupling Terms and Conical Intersections*; Wiley, New York 2006
- (7) Domcke W and Yarkony D R 2012 *Annu. Rev. Phys. Chem.* **63** 325
- (8) Ashfold M N R, Devine A L, Dixon R N, King G A, Nix M G D and Oliver T A A 2008 *PNAS* **105** 12701
- (9) Lim J S and Kim S K 2010 *Nature Chemistry* **2** 627
- (10) Polli D *et al* 2010 *Nature* **467** 440

- (11) Martinez T J 2010 *Nature* **467** 412
- (12) Moiseyev N, Sindelka M and Cederbaum L S 2008 *J. Phys. B* **41** 221001
- (13) Sindelka M, Moiseyev N and Cederbaum L S 2011 *J. Phys. B* **44** 045603
- (14) Halász G J, Vibók Á, Sindelka M, Moiseyev N and Cederbaum L S 2011 *J. Phys. B* **44** 175102
- (15) Halász G J, Vibók Á and Cederbaum L S 2015 *J. Phys. Chem. Lett.* **6** 348
- (16) Csehi A, Halász G J, Cederbaum L S and Vibók Á 2017 *Phys. Chem. Chem. Phys.* **19** 19656
- (17) Seideman T 1995 *J. Chem. Phys.* **103** 7887
- (18) Friedrich B, Herschbach D 1995 *Phys. Rev. Lett.* **74** 4623
- (19) Koch C P, Lemesko M, Sugny D 2018 arXiv:1810.11338
- (20) Yarkony D R 1996 *Rev. of Mod. Phys.* **68** 985
- (21) Galego, J.; Garcia-Vidal, F. J.; Feist, J. Cavity-Induced Modifications of Molecular Structure in the Strong-Coupling Regime. *Phys. Rev. X* **2015**, 5, 1-14.
- (22) Galego J, Garcia-Vidal F J and Feist J 2016 *Nature Comm.* **7** 13841
- (23) Kowalewski M, Bennett K and Mukamel S 2016 *J. Chem. Phys.* **144** 054309
- (24) Kowalewski M, Bennett K and Mukamel S 2016 *J. Phys. Chem. Lett.* **7** 2050
- (25) Bennett K, Kowalewski M and Mukamel S 2016 *Faraday Discuss.* **194** 259
- (26) Hutchison J A, Schwartz T, Genet C, Devaux E and Ebbesen T W 2012 *Angew. Chem. Int. Ed.* **51** 1592
- (27) Schwartz T *et al* 2013 *Chem. Phys. Chem.* **14** 125
- (28) George J *et al* 2015 *Faraday Discuss.* **178** 281

- (29) Zhong X *et al* 2016 *Angew. Chem. Int. Ed.* **55** 6202
- (30) Ebbesen T W 2016 *Acc. Chem. Res.* **49** 2403
- (31) Thomas A *et al* 2016 *Angew. Chem. Int. Ed.* **55** 11462
- (32) Chikkaraddy R *et al* 2016 *Nature* **535** 127
- (33) Galego J, Garcia-Vidal F J and Feist J 2017 *Phys. Rev. Lett.* **119** 136001
- (34) Feist J, Galego J and Garcia-Vidal F J 2018 *ACS Photonics* **5** 205
- (35) Luk H L, Feist J, Toppari J J and Groenhof G 2017 *J. Chem. Theory Comput.* **13** 4324
- (36) Herrera F and Spano F C 2016 *Phys. Rev. Lett.* **116** 238301
- (37) Herrera F and Spano F C 2017 *Phys. Rev. Lett.* **118** 223601
- (38) Herrera F and Spano F C 2018 *ACS Photonics* **5** 65
- (39) Ribeiro R F, Martínez-Martínez L A, Du M, Campos-Gonzalez-Angulo J and Yuen-Zhou J 2018 *Chem. Sci.* **9** 6325
- (40) Martínez-Martínez L A, Ribeiro R F, Campos-González-Angulo J and Yuen-Zhou J 2018 *ACS Photonics* **5** 167
- (41) Du M, Ribeiro R F and Yuen-Zhou J 2018 arXiv:1810.10083
- (42) Flick J, Ruggenthaler M, Appel H and Rubio A 2017 *Proc. Natl. Acad. Sci. U. S. A.* **114** 3026
- (43) Flick J, Appel H, Ruggenthaler M and Rubio A 2017 *J. Chem. Theory Comput.* **13** 1616
- (44) Ruggenthaler M, Tancogne-Dejean N, Flick J, Appel H and Rubio A 2018 *Nat. Rev. Chem.* **2** 0118
- (45) Flick J, Rivera N and Narang P Strong 2018 *Nanophotonics* **7** 1479

- (46) Triana J F, Peláez D and Sanz-vicario J F 2018 *J. Phys. Chem. A* **122** 2266
- (47) Triana J F and Sanz-vicario J L 2019 *Phys. Rev. Lett.* **122** 063603
- (48) Vendrell O 2018 *Chem. Phys.* **509** 55
- (49) Vendrell O 2018 *Phys. Rev. Lett.* **121** 253001
- (50) Csehi A, Halász G J, Cederbaum L S and Vibók Á 2017 *J. Phys. Chem. Lett.* **8** 1624
- (51) Szidarovszky T, Halász G J, Császár A G, Cederbaum L S and Vibók Á 2018 *J. Phys. Chem. Lett.* **9** 6215
- (52) Szidarovszky T, Halász G J, Császár A G, Cederbaum L S and Vibók Á 2018 *J. Phys. Chem. Lett.* **9** 2239
- (53) Meyer H D, Manthe U and Cederbaum L S 1999 *Chem. Phys. Lett.* **165** 73
- (54) Worth G A *et al* The MCTDH package, version 8.4, University of Heidelberg, Germany; <http://mctdh.uni-hd.de/> 2007
- (55) Werner H J, Knowles P J, Knizia G, Manby F R, Schütz M, et al. MOLPRO, version 2015.1, a package of ab initio programs. 2015; see <http://www.molpro.net> (accessed May 11, 2016).
- (56) Tóth A, Badankó P, Halász G J, Vibók Á and Csehi A 2018 *Chem. Phys.* **515** 418
- (57) Bandrauk A D and Sink M L 1978 *Chem. Phys. Lett.* **569** 57

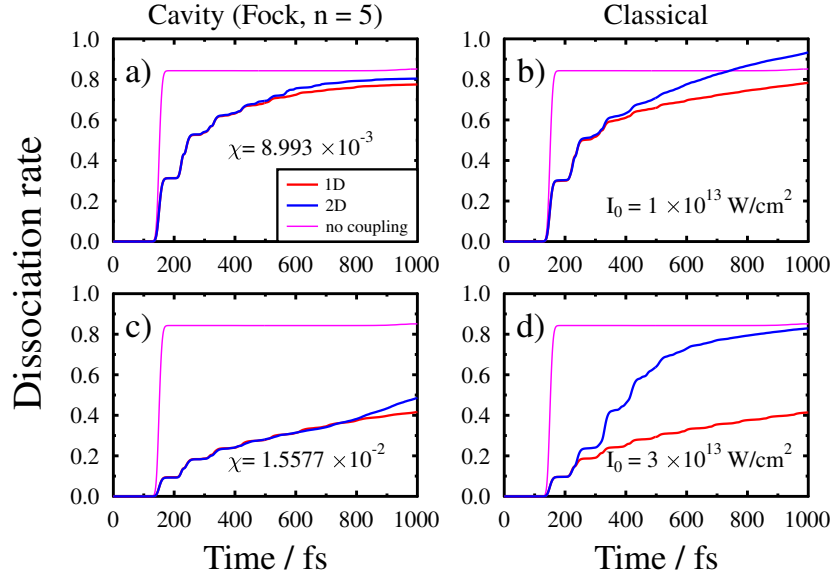


Figure 4: Comparison of the time-dependent ground-state dissociation rates of the LiF molecule modified by quantum and classical laser light. The correspondence between the quantum and classical light results is demonstrated for two different intensities and cavity coupling values. The 1D and 2D dissociation rates are shown by the red and blue lines, respectively. The magenta curves depict the bare results.